3-1-2010

Effects of Crystallographic Orientation on the Early Stages of Oxidation in Nickel and Chromium

Louis P. Bonfrisco
Boise State University

Megan Frary
Boise State University

 DOI: 10.1007/s10853-009-4144-x

EFFECTS OF CRYSTALLOGRAPHIC ORIENTATION ON THE EARLY STAGES OF OXIDATION IN NICKEL AND CHROMIUM

Louis P. Bonfrisco and Megan Frary*

Department of Materials Science and Engineering

1910 University Drive, Boise State University, Boise, ID 83725 USA

*Corresponding author: meganfrary@boisestate.edu, 208-426-1061 (ph), 208-426-2470 (fax)

ABSTRACT

Surface orientation plays an important role in the oxidation behavior of single crystals where studies have found the relative oxidation rates for surfaces with different orientations. However, most materials are polycrystalline and contain myriad orientations that contribute to the overall oxidation process. Here we determine the effects of orientation on the early stages of oxidation behavior as a function of surface orientation for polycrystalline nickel (face-centered cubic) and chromium (body-centered cubic). After high temperature oxidation, the oxide topography is characterized using optical profilometry and the underlying microstructure is characterized with electron backscatter diffraction (EBSD). By correlating results from EBSD and optical profilometry, the oxide height is determined for each crystallographic orientation. In both Ni and Cr, a strong relationship is observed between the oxidation rate and direction of the surface normal; for Ni, (111) surfaces oxidize slowest, while (100) surfaces in Cr have the lowest oxidation rates. Although orientation-dependent oxidation rates are observed at short times, the effect is diminished at longer oxidation times.

Keywords: EBSD, oxidation, surface orientation

1. INTRODUCTION

Although many studies of oxidation neglect the effects of the underlying microstructure (e.g., grain size, grain boundary character, and crystallographic orientation), surface orientation has been shown to impact the rate of oxidation in both Ni and Cu alloys [1-8]. The dependence of oxidation rate on crystallographic orientation has also been suggested for Fe and Cr [9-14]. In oxidation studies on Ni single crystals, more rapid oxidation is consistently observed on (001) faces than on (111) faces [3-8]. In those studies, where oxidation occurs for up to hundreds of hours, the character of the grain boundaries that form in the oxide is responsible for the observed differences in oxidation rate. Oxides grown on (111) surfaces tend to form fewer grain boundaries because the epitaxial growth relationship (i.e., $(111)_{Ni}||(111)_{NiO}$) has only two variants in oxide alignment. However, oxides grown on the (001) face, which also have an epitaxial relationship (i.e., $(001)_{Ni}||(111)_{NiO}$), form more grain boundaries because there are four oxide alignments possible [3, 5, 6]. A higher concentration of grain boundaries, which are known to exhibit higher diffusivities than the bulk [15], is responsible for the observed differences in oxidation rate. More recent studies have estimated the grain boundary character distribution in NiO based on experimentally determined orientation distribution functions of the oxide [8, 16]. Oxides grown on the (111) faces were found to contain significantly lower fractions of general high-angle grain boundaries than those grown on the (001) faces –

47% vs. 99% of high-angle boundaries [16]. While the (111) and (001) faces have been studied extensively, the (011) has received considerably less attention. In general, the (011) face is found to form an oxide that is polycrystalline and contains many more high diffusivity paths (e.g., high-angle grain boundaries and dislocations) than do the oxides on (001) and (111) faces [3, 6]. In addition, oxidation of the (011) surface has been shown to be most sensitive to effects of surface contamination [6]. In previous work by Graham *et al.*, the oxidation of single crystal orientations was explicitly compared to that of polycrystalline Ni; the (112) and (111) planes had lower oxidation rates than the polycrystalline sample, but (001) surfaces had a higher oxidation rate than the polycrystal [5]. Their work suggests the averaging effect all orientations have on the rate of oxidation.

Orientation effects on oxidation rate have also been observed in other single crystal systems. For example, Young *et al.* found that the oxidation rate of Cu at temperatures from 70 to 178°C increases with surface orientation as (311) < (110) < (111) < (100) [2]. In contrast, Rhodin *et al.* found the oxidation rate of Cu at 900°C to be faster on the (110) surface than the (111) surface [1]. The different results found by these authors suggest that not only does the orientation affect the oxidation rate and possibly the mechanism as well, but so too does the temperature. For Cr, work by Caplan and Sproule [14] has shown that some orientations of Cr lead to the growth of a thin, monocrystalline oxide, whereas others developed a thicker, polycrystalline oxide. However, the orientations that lead to each behavior were not identified.

In addition to the studies on single crystals described above, recent work has evaluated corrosion or oxidation rates on polycrystalline specimens in which the effect of orientation is determined over the entire range of possible surface orientations. A novel experimental technique was developed in 2003 by Schuh *et al.* in which electron backscatter diffraction (EBSD) was used to determine the surface orientation of a polycrystalline specimen and atomic force microscopy (AFM) was used to characterize surface height after corrosion [17]. In polycrystalline Inconel 600, the corrosion rate increased according to the pattern: (111) < (011) < (001). Moreover, the relationship between corrosion depth and the angle between the surface normal and the [111] direction was linear. In a similar study, Gray *et al.* exposed the surface of Ni-based alloy 22 to hydrochloric acid at 1 and 3 M [18]. At the lower concentration, the results match those in Ref. [17]; however, at the higher concentration, corrosion depth follows the pattern: (111) < (001) < (011). Schreiber *et al.* applied the technique developed in [17] to study the influence of grain orientation on corrosion of α-iron [19]. The corrosion rate was greatest for (111) and (101) orientations (referred to by the authors as close packed planes), while orientations close to the (001) plane resisted corrosion [19]. Finally, Diamanti *et al.* have used EBSD and optical microscopy to determine the orientation dependence of anodization of titanium [20].

From the single crystal and polycrystal studies described here, it is clear that the orientation effects on oxidation are complex and not well understood. In both Cu, Ni and their alloys, the oxidation mechanism and effects of orientation depend on temperature [1, 2, 4, 21-24]. The grain size of the oxide has also been shown to lead to different oxidation rates in polycrystalline Ni [15, 25]. Furthermore, oxidation behavior depends on the crystal structure of the material (e.g., different results are found in face-centered and body-centered cubic metals). In the current work, we apply the procedure developed in Ref. [17] to study the orientation dependence of oxidation in polycrystalline Ni (fcc) and Cr (bcc) at short oxidation times. To the best of our knowledge, this represents the first time that high temperature oxidation behavior has been studied over the entire spectrum of crystallographic

orientations. We compare the results of our work to those obtained during single crystal oxidation studies and polycrystalline corrosion experiments.

2. Experimental procedures

The materials used for the present work were high purity Ni (99.995%) and Cr (99.95%) which were obtained from Southern Tool Steel (Chattanooga, TN) and Kurt J. Lesker (Clairton, PA), respectively. The Ni was in the form of a square bar with a cross-sectional area of 2.5 × 2.5 cm^2 and the Cr was in the form of a disk with a diameter of 2.5 cm and thickness of 6 mm. Specimens for oxidation treatments were cut from the as-received materials; Ni specimens had a thickness of 3 mm, while Cr specimens were cut to be one quarter of the original disk. To ensure that there was no residual strain from processing, the as-received specimens were annealed in air (40 min at 1100°C for Ni, 120 min at 1000°C for Cr) prior to subsequent oxidation steps. To investigate the effects of grain size on oxidation rate, a second set of specimens was cut from the as-received Ni (thickness = 3 mm); these were annealed at 1100°C for 15, 55 and 100 min in air to produce different grain sizes.

In order to characterize the rate of oxidation on individual grains, it is important that all grains start out at the same height. To this end, prior to oxidation treatments specimens were mechanically ground to remove any oxide layer that formed during annealing and then polished flat using standard metallographic techniques including a final polish with 0.02 μm non-crystallizing colloidal silica. Atomic force microscopy and optical profilometry were used to ensure that the surface was sufficiently smooth; surface roughness was found to be less than 30 nm. Specimens were oxidized in a MTI OTF-1200X tube furnace with compressed air flowing over the sample at a rate of 60 mL/min. Ni specimens that were annealed for 40 min were oxidized at 700°C for 5, 10 and 15 min, while Cr specimens were oxidized at 950°C for 2 min. Ni specimens that had been annealed to have different grain sizes were oxidized at 700°C for 15 min. The mass of the specimens with varying grain size was determined before and after oxidation using a Denver Instruments balance with 10 μg precision.

After the high temperature oxidation step, the surface topography of the specimens was characterized with a Veeco optical profiler whose vertical resolution is 3 nm. For each specimen, approximately 15-20 areas (each approximately 1.2 × 0.9 mm^2) were imaged with optical profilometry. After characterization of the oxide surface height, the oxide was carefully polished off to reveal the underlying grain structure on which the oxide had grown. The crystallographic texture and grain boundary character of the metal substrate were determined using EBSD and Orientation Imaging Microscopy (OIM™). The TSL/EDAX (Mahwah, NJ) EBSD system is mounted on a LEO 1430VP SEM and an operating voltage of 25 kV was used. Crystallographic data were collected on a standard hexagonal grid with a step size between 10-12 μm on areas approximately 1 × 1 mm^2. The areas selected for EBSD analysis matched up with those where oxide height was also measured.

After both the optical profiler and EBSD data had been collected, average crystallographic orientation, height and roughness could be determined for each unique grain within the sampled areas. The average grain orientation was found first by manually selecting three points from within the grain at random and taking an average; in this way, the orientation spread was found to be less than 1°. A cleaning algorithm was then applied to the data set whereby the average grain orientation was assigned to all points within the grain. To determine the average

surface height of the grain, an area average was performed using the Veeco optical profiler software; depending on the grain shape, either a circle or rectangle was used to maximize the area used in averaging. The average roughness of each grain was found in a similar manner and provides a good estimate of the "error" associated with the average height measurement. The difference between maximum and minimum grain height in an area was typically greater than 400 nm while the average roughness values were between 0 and 60 nm.

3. RESULTS

3.1. GRAIN SIZE DEPENDENCE OF OXIDATION

To determine the relative effect of grain size on oxidation rate, three specimens were produced that had the same random crystallographic texture but varied grain size. Using the OIM™ Analysis software, the grain sizes (mean linear intercept) were found to be 115, 212 and 329 μm with corresponding special boundary length fractions of 0.45, 0.45 and 0.30. The effect of grain size on oxidation rate is illustrated in Figure 1 where the mass change per unit area is shown as a function of grain size after oxidation for 15 min at 700°C. These oxidation conditions were chosen to match those used in studying the orientation dependence of oxidation. Three experiments were performed for each grain size and the data in Figure 1 represent the average values from the three experiments. Although the error bars are relatively large, Figure 1 shows that increasing substrate grain size results in a decrease in oxidation rate.

3.2. ORIENTATION-DEPENDENT OXIDATION OF NI

In order to characterize the orientation dependence of oxidation, the surface orientation and oxide height had to be determined for the same areas on the specimen. By scanning areas using a pre-determined pattern, it was possible to identify identical areas for both EBSD and optical profiler analysis. Figure 2 shows a pair of images for a single area from the Ni specimen oxidized for 5 min at 700°C; several grains are labeled (a through e) which are easily identified in both maps. In the EBSD map, color corresponds to crystallographic orientation, while in the optical profiler map, color corresponds to oxide surface height. In Figure 2, the orientation-dependence of oxidation can be observed qualitatively; grains whose surface normals are nearer <111> (e.g., grain e) have lower surface heights, or oxide thicknesses, than do grains with normals near <100> (e.g., grain b). The single area shown in Figure 2 contains ~ 50 grains, and 9 to 12 such areas were collected for each Ni specimen annealed 5, 10 and 15 min at 700°C.

For each grain that can be uniquely identified in the EBSD and optical profiler scans for an area, the crystallographic orientation and average relative surface height are determined. In Figure 3, the relative oxide height, Δh, which has been normalized to the lowest grain in the scan area, is shown as a function of crystallographic orientation for each of the three oxidation times. The location of the point inside the standard stereographic triangle gives the orientation of the grain and the color of the point indicates the relative oxide height. Although 9 to 12 areas were analyzed for each specimen, only four representative areas are included in the interest of space. In each case, the oxide height is found to be greatest for orientations near the <100> direction and lowest for orientations near the <111> direction, although the strength of the trend varies.

Using the same approach as Schuh *et al.* [17], the oxidation rate is plotted as a function of the deviation of the surface normal from the <111> direction in Figure 4 for the same areas shown in Figure 3. Although some areas show significant scatter in the data, there is clearly a relationship between oxidation rate and the surface normal direction. It is important to note that the range in relative oxide height decreases with increasing oxidation time; as we are measuring the surface height with respect to the lowest grain in the scan area, this result corresponds to oxides that show a weaker dependence on surface orientation with increasing oxidation time.

3.3. Orientation-dependent oxidation of Cr

The orientation-dependence of oxidation for pure Cr was determined in a manner identical to that for Ni. Figure 5 shows the EBSD and optical profiler maps for the same area from the Cr specimen oxidized for 2 min at 950°C. Again, excellent correlation between the two images can be observed. However, in contrast to trends observed for Ni, Cr grains whose surface normals are nearer <111> (e.g., grain e) show greater surface heights than do grains whose normals are near <100> (e.g., grain b). As in Figure 3, the effect of orientation on oxidation behavior is illustrated in Figure 6 for Cr where the location of the point in the standard stereographic triangle gives the orientation of the grain and the color of the point indicates the relative oxide height. As Figure 5 showed qualitatively, the trend toward lower oxidation rates for surface normals near <100> is also borne out in Figure 6. The relative oxide height as a function of the angle between the surface normal and the <100> direction is shown in Figure 7. Again, although some areas show scatter in the data, the relationship is quite apparent.

4. Discussion

4.1. Grain size dependence of oxidation

The grain size dependence of oxidation was described in the previous section. Three specimens that had different grain sizes but similar textures and grain boundary character distributions underwent identical oxidation treatments. Given that the grain size was the only microstructural variable that differed among the three, changes in oxidation rate can be attributed to a grain size effect. An increase in the total grain boundary length at the surface corresponds to an increase in the available high diffusivity paths for ion transport; this microstructural effect on oxidation rate has been suggested previously [5, 6, 9, 16, 26-28]. The effect of grain size (or total grain boundary length) on oxidation rate may also be evident in the studies of orientation effects in polycrystals. For example, in Fig. 4 (area Ni5a), considerable scatter in relative oxide height is observed for grains whose normal directions lie within narrow angular ranges; the scatter may be attributed to grains of different sizes oxidizing at different rates.

4.2. Orientation dependent oxidation in fcc metals

The orientation dependence of oxidation rate was investigated for nickel at times ranging from 5 to 15 min. The data consistently show a trend indicating that as the underlying crystallographic orientation deviates away from the reference direction of <111> the oxidation rate increases. The results obtained here for oxidation of Ni at 700°C are generally in agreement with single crystal studies that consistently show more rapid oxidation on (001) faces than on (111) faces [3-8]. In addition, the relationship (111) < (011) < (001) was observed for oxidation of single crystal Ni at 500 and 600°C [4] and for corrosion of Ni-based superalloys at low acid concentrations where a passivating film forms [17, 18]. During high temperature oxidation, oxide growth is expected to start with the

nucleation and lateral growth of the film within grains and continue with growth of the oxide normal to the film surface [10, 16]; therefore, it is not surprising that oxide thickness at short times would follow the same pattern as observed for oxidation studies on single crystals.

Another important result from the present work is that with increasing oxidation time, the relative importance of crystallographic orientation on oxidation rate diminishes. In contrast, single crystal studies show that differences in the rate of oxidation for different surface orientations persist up to at least 24 hours of oxidation [10, 12, 16, 27]. Two different approaches are used to quantify the diminishing effects of substrate orientation on oxidation rate in Ni. First, the maximum relative oxide height, Δh_{max}, was determined for each area at all oxidation times. Figure 8a shows Δh_{max} as a function of oxidation time where the circles represent the values from individual areas and the squares are the average values for each oxidation time. In our study of polycrystalline nickel, Δh_{max} decreased from 444 to 264 nm as oxidation time increases from 5 to 15 min; after 30 min of oxidation, no change in oxide height could be measured. The data point at 30 min is a result of a number of oxidation experiments where no height differences could be resolved. It is clear from Fig. 8a that the effect of surface orientation becomes weaker with increasing time. It is important to note that only the relative oxide height is decreasing with time, not the overall oxide thickness. The second approach to quantifying the effects of orientation on oxidation considers changes to the slope of a linear fit to the data presented in Figure 4. The orientation strength, $\Delta h/\Delta\theta$ (where θ is the angle in degrees between the surface normal and the <111> direction), is determined for every area at each oxidation time. The oxidation strength is plotted as a function of oxidation time in Figure 8b where the circles represent the values from individual areas and the squares are the average values for each oxidation time. The results in Figure 8b show further that not only does the maximum relative oxide height change, but the linear trend remains with decreasing slope. Although the results in Figures 8a and b look similar, they are not identical because the grain with $\Delta h = 0$ has a slightly different orientation in each area which can lead to a different value of $\Delta h/\Delta\theta$ for the same Δh_{max}.

The results in Figure 8 suggest that during the initial stages of oxidation in polycrystalline materials, the underlying surface orientation is the dominant factor in determining oxide thickness. However, as the oxide thickness increases, the surface orientation becomes less of a factor and other aspects of the oxide structure control the rate of polycrystal oxidation. Since oxidation of Ni occurs at the oxide-gas interface, surface orientation can be expected to play a role only in the thinnest oxide films. In addition, were anisotropic growth to continue, differences in surface height would be magnified with increased oxidation time. Such uneven surfaces would be energetically unfavorable and could drive processes that would tend to override the effects of surface orientation on oxidation.

4.3. Orientation dependent oxidation in bcc metals

The oxidation rate for chromium was investigated at 950°C for 2 min and was found to increase as the surface normal direction deviates away from the <001>. It is somewhat unexpected that <001> has the lowest oxidation rate and acts as the reference direction since it is not the closest packed plane in bcc structures. Unlike Ni where oxidation studies of single crystals are abundant, no such studies exist for Cr with which to make comparisons. However, Cr_2O_3 has a $R\bar{3}c$ crystal structure and its diffusivity, a second-rank tensor property, is expected to be

anisotropic, which could contribute to differences in oxide growth rate for surfaces with different orientations. As with Ni, the maximum relative oxide height decreased with increasing oxidation time; no resolvable differences in oxide height could be observed after 5 min. This phenomenon occurs more quickly in Cr than in Ni, indicating that the effect of substrate orientation on oxidation may be less important or that diffusion through oxide grain boundaries is more effective [14].

5. Conclusions

In the present work, we have studied the orientation-dependence of the early stages of oxidation in nickel (fcc) and chromium (bcc). The experimental method developed by Schuh *et al*. [17] for rapid characterization of the effects of surface orientation on corrosion was adapted to study high temperature oxidation. By using optical profilometry to characterize surface height, significantly larger data sets could be acquired more quickly than if using AFM, allowing for a better understanding of the role surface orientation plays in oxidation behavior. The main conclusions of this work are:

1. The oxidation rate for nickel was measured for hundreds of different orientations and found to increase with surface orientation as (111) < (011) < (001). Furthermore, the rate of oxidation was shown to increase as the surface normal direction deviated away from <111>. Scatter in the data is attributed to grains of similar orientations having different grain sizes.

2. The oxidation rate for chromium was also measured for more than 100 unique orientations. The rate was found to increase as (001) < (011) < (111). In the case of Cr, the rate of oxidation increased as the surface normal deviated from <001>.

3. For both Ni and Cr, the orientation-dependence of oxidation rate was only evident for short oxidation times. This effect was quantified for Ni wherein the maximum height difference between grains was found to decrease with increasing oxidation time. For oxidation times greater than 30 min, no effect of orientation on oxidation rate could be measured. In Cr, the orientation-dependence exists for oxidation times less than 5 min.

Acknowledgements

This work was supported in part by DOE contract number DE-AC07-05ID14517 administered through the Center for Advanced Energy Studies, Idaho Falls, ID. LPB was supported in part by a fellowship from the NASA Idaho Space Grant Consortium. MF acknowledges the support of the United States National Science Foundation under grant number 0642363.

REFERENCES

1. Rhodin TN, Jr. (1950) J. Appl. Phys. 21:971.
2. Young FW, Jr., Cathcart JV, Gwathmey AT (1956) Acta Metall. 4:145.
3. Cathcart JV, Peterson GF, Sparks CJ (1969) J. Electrochem. Soc. 116:664.
4. Herchl R, Khoi NN, Homma T, Smeltzer WW (1972) Proceedings of the Soil Science Society of America 4:35.
5. Graham MJ, Hussey RJ, Cohen M (1973) J. Electrochem. Soc. 120:1523.
6. Khoi NN, Smeltzer WW, Embury JD (1975) J. Electrochem. Soc. 122:1495.
7. Czerwinski F, Szpunar JA (1998) Acta Mater. 46:1403.
8. Czerwinski F, Zhilyaev A, Szpunar JA (1999) Corros. Sci. 41:1703.
9. Atkinson A (1985) Rev. Mod. Phys. 57:437.
10. Kofstad P, Proceedings of the 1983,vol. 123.
11. Lawless KR (1974) Rep. Prog. Phys. 37:231.
12. Peraldi R, Monceau D, Pieraggi B (2002) Oxid. Met. 58:275.
13. Sarrazin P, Galerie A, Caillet M (1996) Oxid. Met. 46:299.
14. Caplan D, Sproule GI (1975) Oxid. Met. 9:459.
15. Li H, Czerwinski F, Zhilyaev A, Szpunar JA (1997) Corros. Sci. 39:1211.
16. Li H, Czerwinski F, Szpunar JA (2001) Defect. Diffus. Forum 194-199:1683.
17. Schuh CA, Anderson K, Orme C (2003) Surf. Sci. 544:183.
18. Gray JJ, El Dasher BS, Orme CA (2006) Surf. Sci. 600:2488.
19. Schreiber A, Schultze JW, Lohrengel MM, Karman F, Kalman E (2006) Electrochimica Acta 51:2625.
20. Diamanti MV, Pedeferri MP, Schuh CA (2008) Metall. Mater. Trans. A 39:2143.
21. Essuman E, Meier GH, Zurek J, Hansel M, Singheiser L, Norby T, Quadakkers WJ (2008) J. Mater. Sci. 43:5591.
22. Sharma SK, Strunskus T, Ladebusch H, Zaporojtchenko V, Faupel F (2008) J. Mater. Sci. 43:5495.
23. Thery PY, Poulain M, Dupeux M, Braccini M (2009) J. Mater. Sci. 44:1726.
24. Gleeson B, Mu N, Hayashi S (2009) J. Mater. Sci. 44:1704.
25. Caplan D, Graham MJ, Cohen M (1972) J. Electrochem. Soc. 119:1205.
26. Czerwinski F, Szpunar JA (1999) Corros. Sci. 41:729.

27. Larsen DE, Jr. (1987) Scripta Metall. 21:1379.

28. Monceau D, Pieraggi B (1998) Oxid. Met. 50:477.

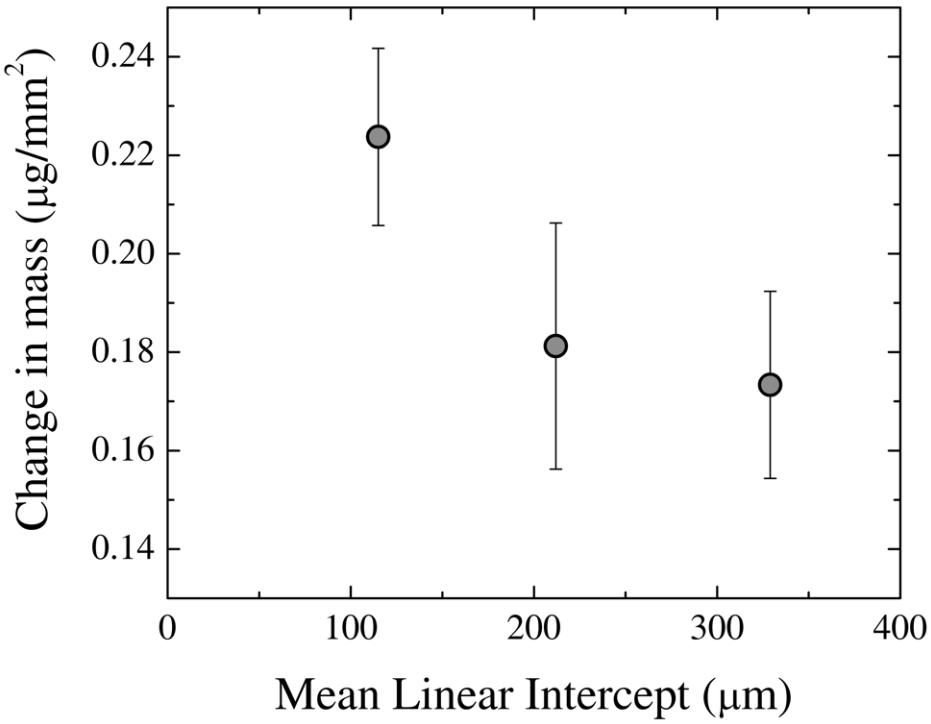

Figure 1: Dependence of the oxidation rate (as measured by mass gain per unit area) on the grain size of the Ni substrate.

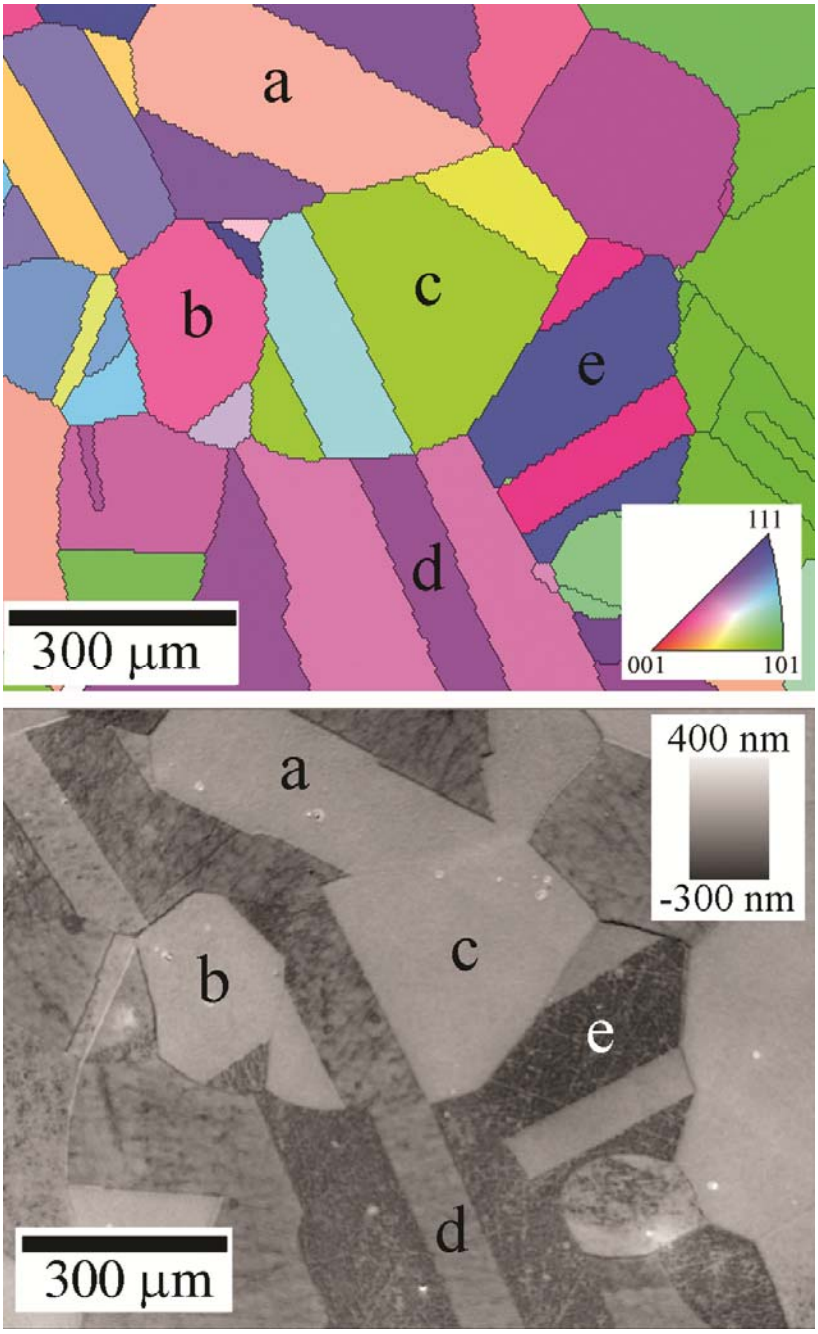

Figure 2: EBSD map (top) that shows crystallographic orientation of Ni and optical profiler image (bottom) that shows the surface height of the oxide after oxidation for 5 minutes at 700°C. Grains labeled *a* through *e* show the two images are indeed of the same area (Ni5g) on the specimen. The inset to the EBSD map shows the relationship between grain color and orientation of the surface normal, while the inset to the optical profiler map shows the relationship between color and surface height.

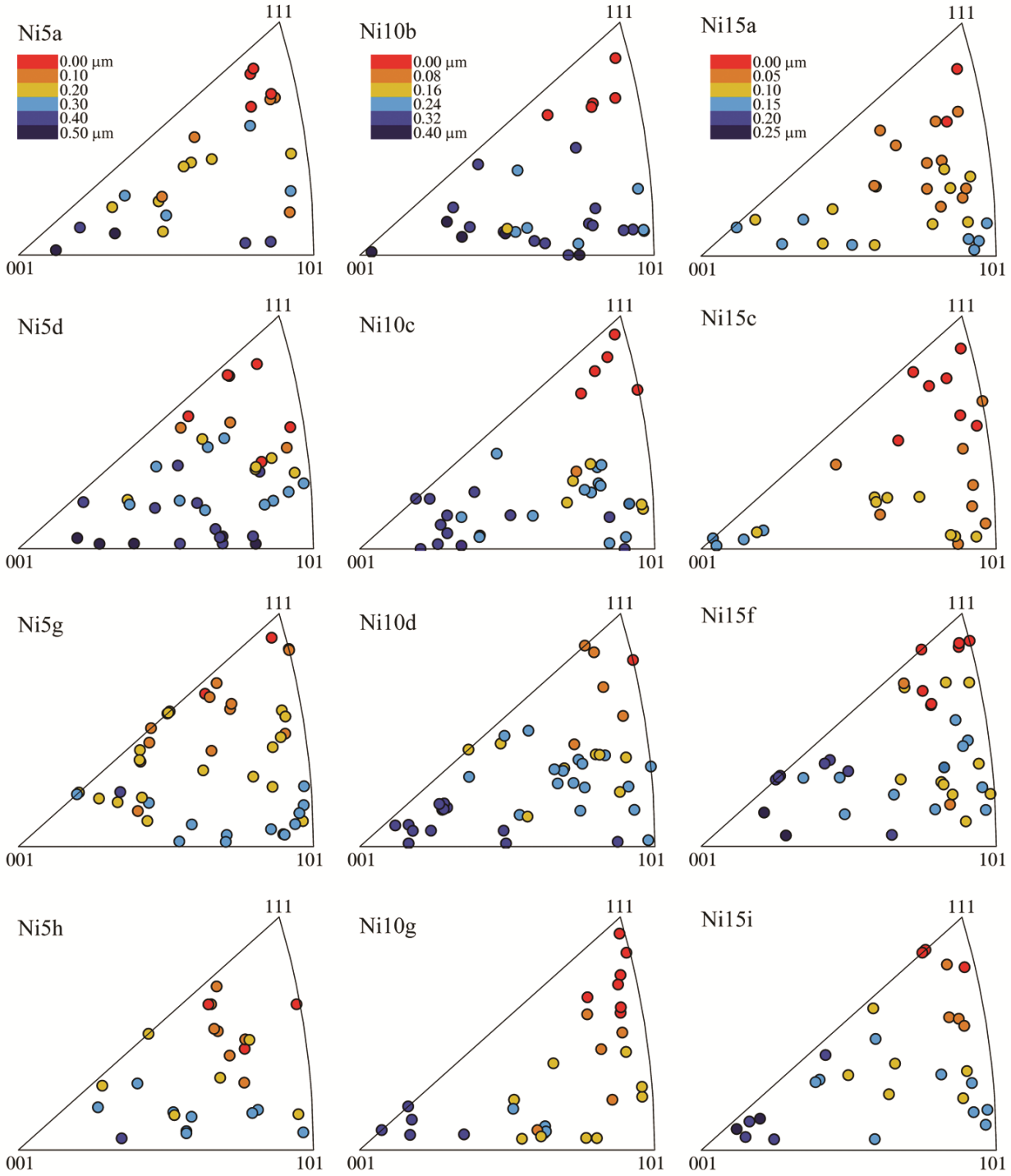

Figure 3: Relative oxide height (indicated by the color of the point) is plotted as a function of crystallographic orientation for Ni oxidized for 5 minutes (left), 10 minutes (middle) and 15 minutes (right) at 700°C. Each point represents a single grain within the scan area and the location of the point inside the inverse pole figure gives the direction of the surface normal.

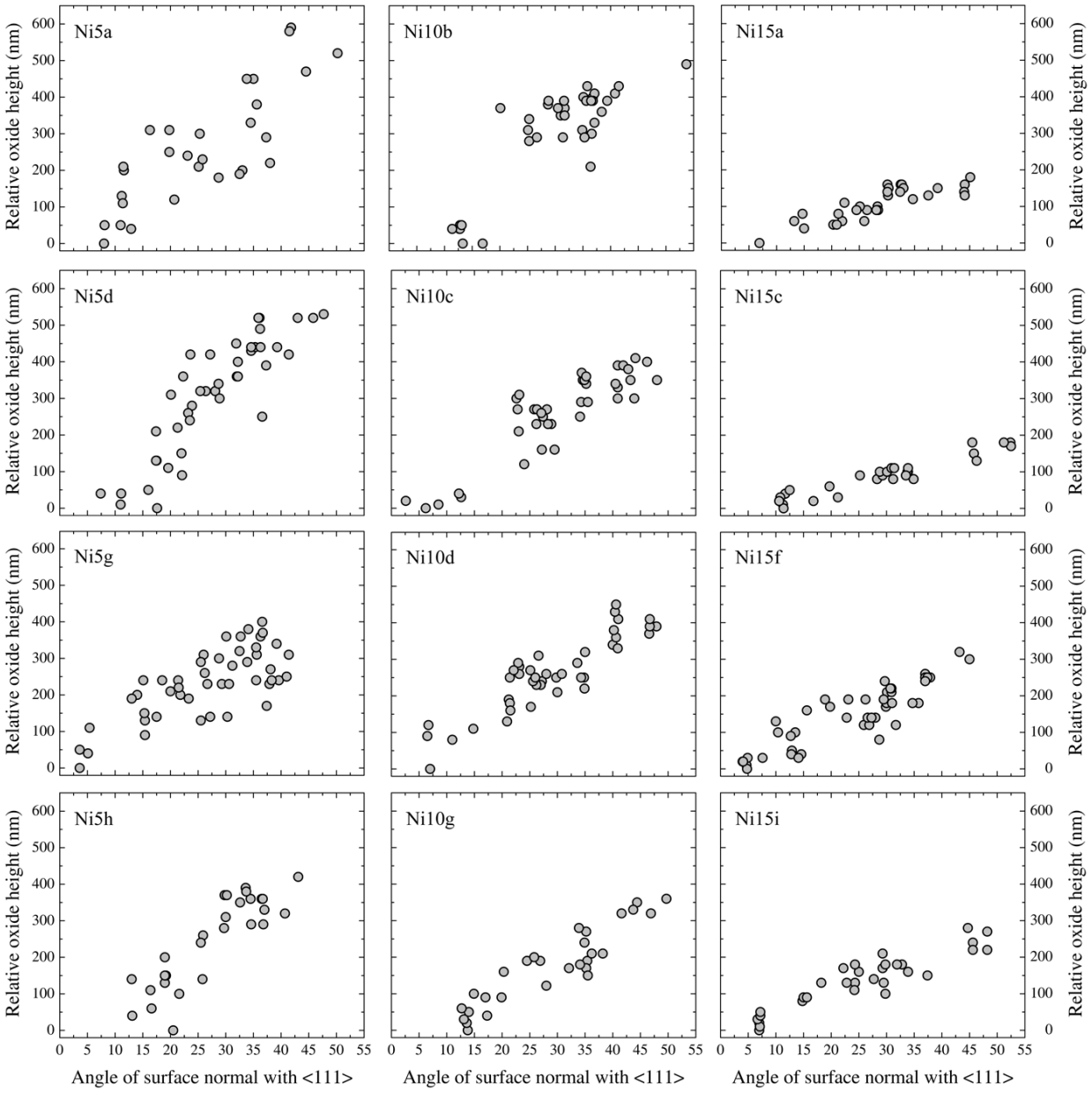

Figure 4: Relative oxide height is plotted as a function of the angle between the surface normal of a grain and the [111] direction for Ni oxidized for 5 minutes (left), 10 minutes (middle) and 15 minutes (right) at 700°C. Each point represents a single grain within the scan area.

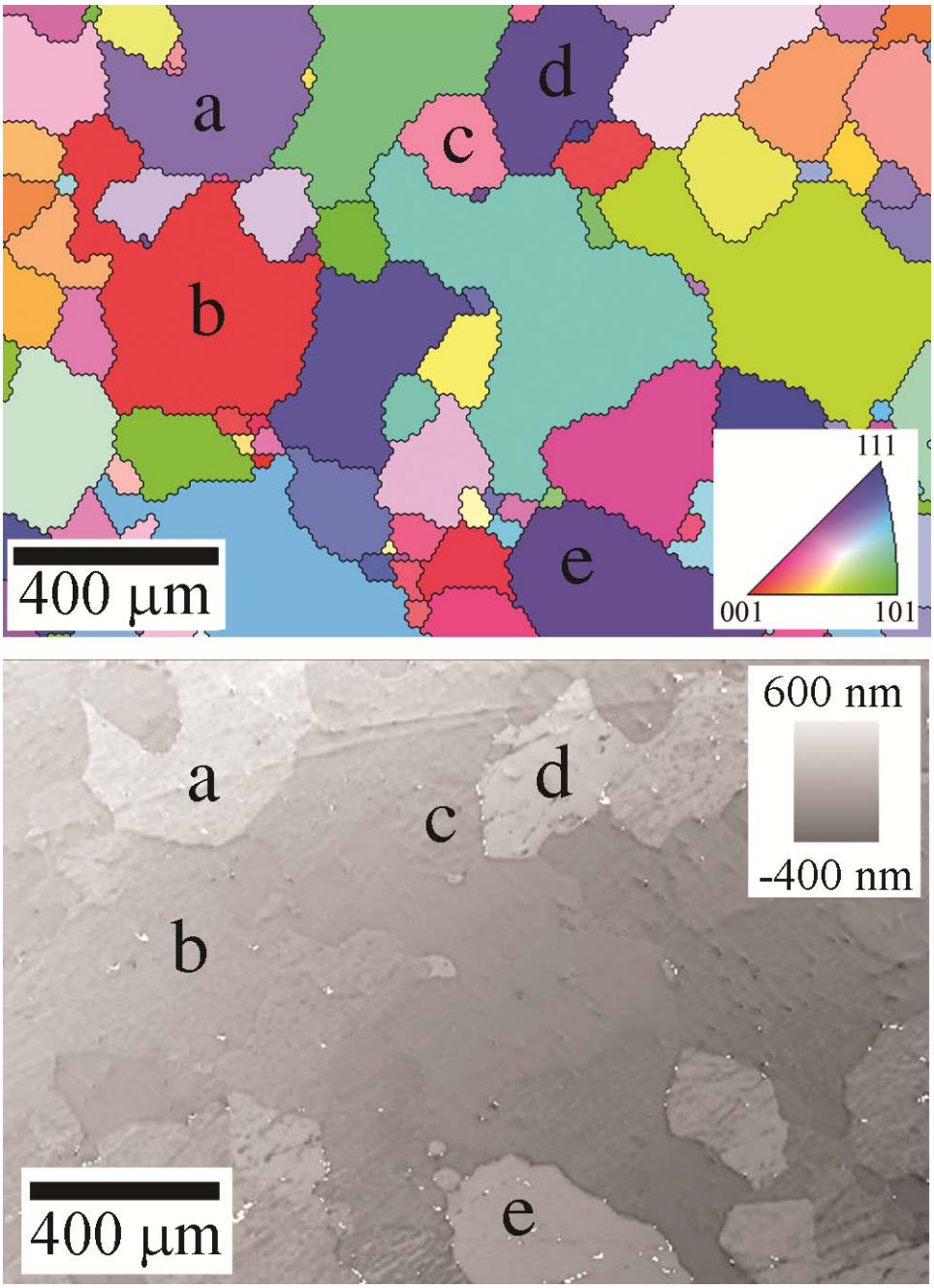

Figure 5: EBSD map (top) that shows crystallographic orientation of Cr and optical profiler image (bottom) that shows the surface height of the oxide after oxidation for 2 min at 950°C. Grains labeled *a* through *e* show the two images are indeed of the same area (Cr2f) on the specimen. The inset to the EBSD map shows the relationship between grain color and orientation of the surface normal, while the inset to the optical profiler map shows the relationship between color and surface height.

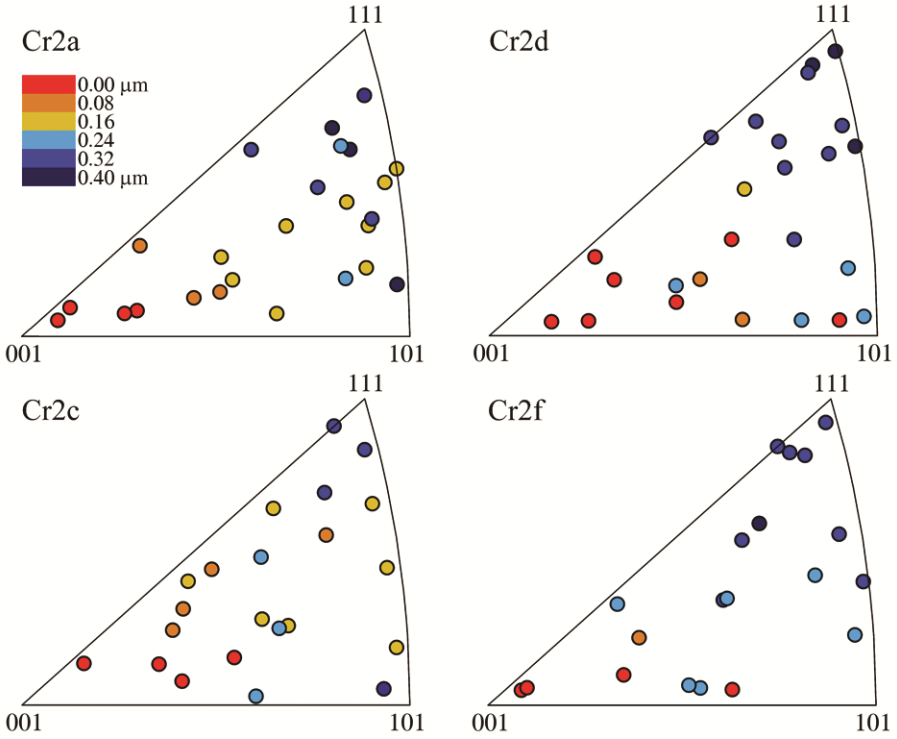

Figure 6: Relative oxide height (indicated by the color of the point) is plotted as a function of crystallographic orientation for Cr oxidized for 2 minutes at 950°C. Each point represents a single grain within the scan area and the location of the point inside the inverse pole figure gives the direction of the surface normal.

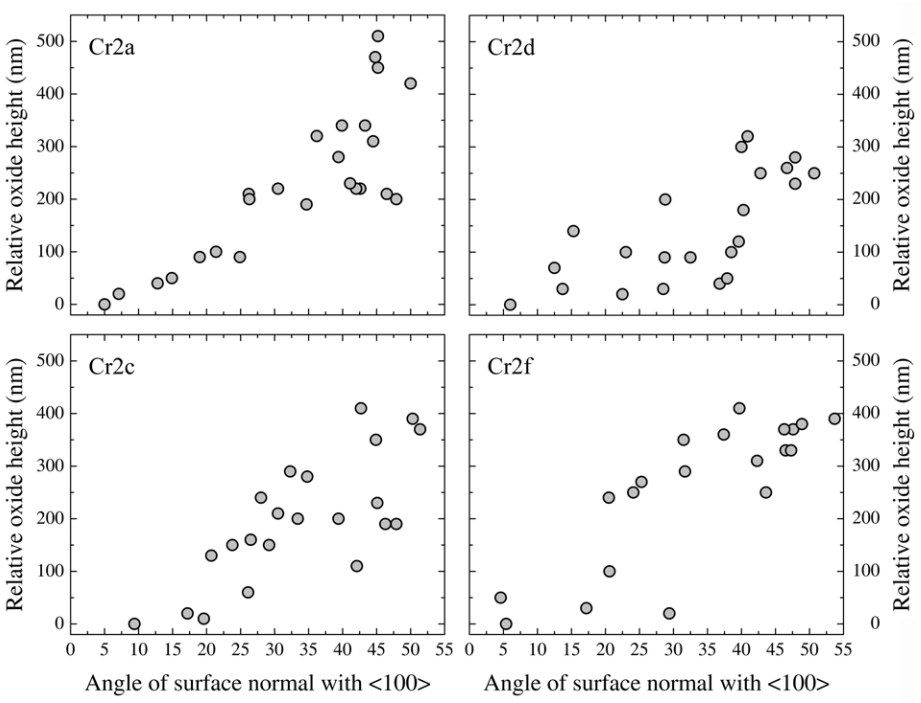

Figure 7: Relative oxide height is plotted as a function of the angle between the surface normal of a grain and the [100] direction for Cr oxidized for 2 minutes at 950°C. Each point represents a single grain within the scan area.

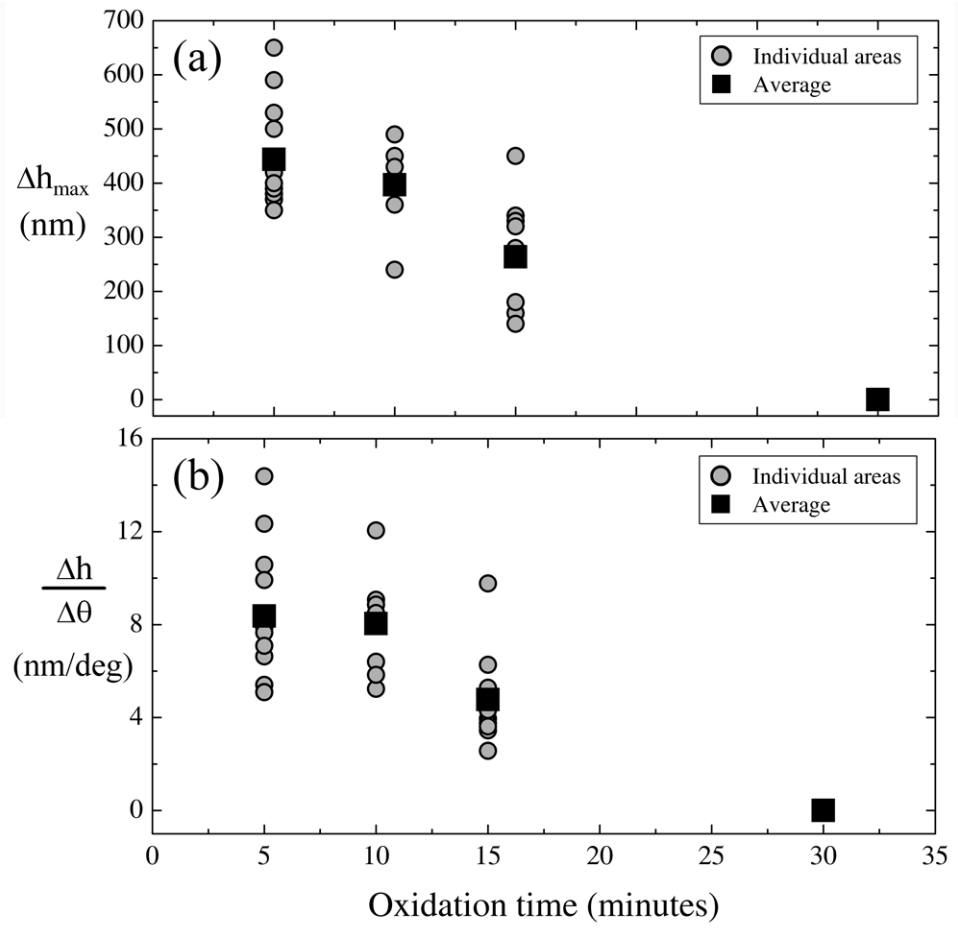

Figure 8: (a) The maximum relative oxide height, Δh_{max}, and (b) the orientation strength, $\Delta h/\Delta\theta$ (i.e., the slope of a linear fit to the data in Fig. 4) are plotted as a function of oxidation time for Ni. Each circle represents the value from a single scan area and the square represents the average of all values at a given oxidation time.